Micro and Nano Systems Letters

LETTER Open Access

All-soft multiaxial force sensor based on liquid metal for electronic skin

Kyuyoung Kim[1], Junseong Ahn[1,2], Yongrok Jeong[2], Jungrak Choi[1], Osman Gul[1] and Inkyu Park[1*]

Abstract

Electronic skin (E-skin) capable of detecting various physical stimuli is required for monitoring external environments accurately. Here, we report an all-soft multiaxial force sensor based on liquid metal microchannel array for electronic skin applications. The proposed sensor is composed of stretchable elastomer and Galinstan, a eutectic gallium-indium alloy, providing a high mechanical flexibility and electro-mechanical durability. Liquid metal microchannel arrays are fabricated in multilayer and positioned along a dome structure to detect multi-directional forces, supported by numerical simulation results. By adjusting the height of the dome, we could control the response of the multiaxial sensor with respect to the deflection. As a demonstration of multiaxial force sensing, we were able to monitor the direction of multidirectional forces using a finger by the response of liquid metal microchannel arrays. This research could be applied to various fields including soft robotics, wearable devices, and smart prosthetics for artificial intelligent skin applications.

Keywords: Electronic skin, Force sensor, Multiaxial sensor, Liquid metal, 3D printing

Introduction

Human skin can detect and understand various mechanical stimuli using multilayered and array structures of mechanoreceptors [1, 2]. Many researchers have recently reported various types of electronics skins (E-skin) mimicking versatile functions of skins such as pressure sensing [3–6], tactile sensing [7, 8], and temperature sensing [9]. To understand the external environments or stimuli in an accurate manner, E-skin should perceive various mechanical information emulating human perception and natural touch. Previously many flexible tactile sensors that solely measure normal [10, 11] or shear forces [12, 13] have been reported. At the interface of the skin, however, not only normal force but also tangential force is experienced, resulting multiaxial forces to the skin. For the dexterous manipulation of objects and thorough understanding of the dynamics at the interfaces, the monitoring of multidirectional forces is essential.

Currently, various multiaxial force sensors have been reported for E-skin applications using MEMS-based metal strain gauges [14, 15]. However, these sensors are limited by their rigid silicon substrate and their adaptability on the soft human skin. Thus, there have been multiaxial force sensors using conductive yarns [16, 17], carbon nanotubes [18, 19] and metal nanowires [20, 21] with flexible substrates like polydimethylsiloxane (PDMS) and Ecoflex. However, solid-state electronics employing metal film, carbon nanotubes, etc. have a limited stretchability and signal drifting in their long-term use. Also, the signals are easily affected by external environmental conditions like temperature and humidity, limiting their applications in real-life.

In this research, we introduce a liquid metal (LM)-based soft multiaxial force sensor for E-skin applications. Detection of multiaxial force was achieved by the implementation of multiple liquid microchannels with 3D dome structure (Fig. 1a). Four LM microchannels were fabricated on the top elastomer layer and the other four

*Correspondence: inkyu@kaist.ac.kr
[1] Department of Mechanical Engineering, Korea Advanced Institute of Science and Technology (KAIST), 291 Daehak-ro, Yuseong-gu, Daejeon 34141, Republic of Korea
Full list of author information is available at the end of the article

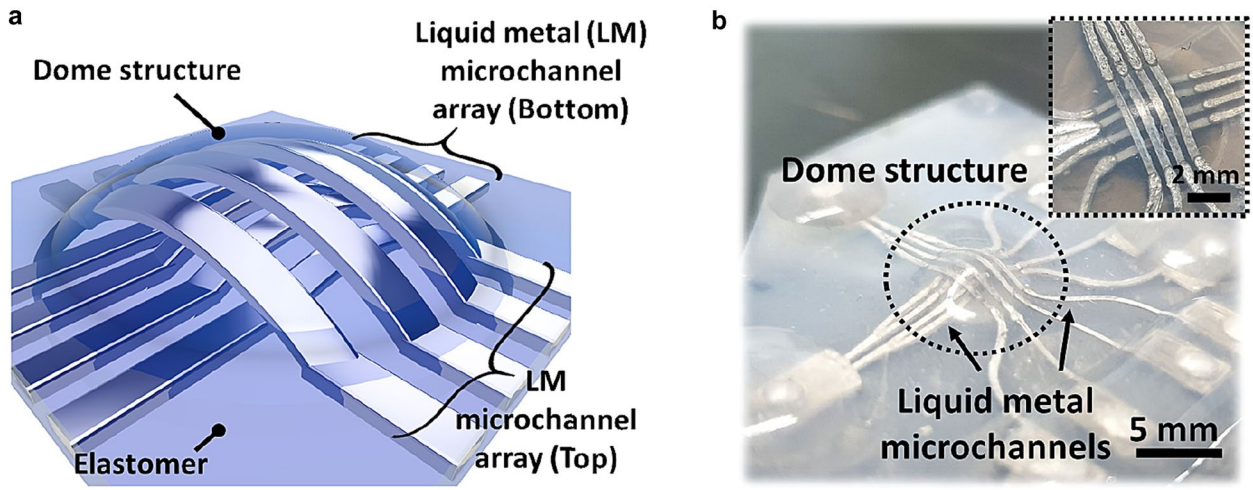

Fig. 1 Liquid metal-based multiaxial force sensor with dome structure. **a** Schematic design of the proposed sensor. **b** Images of the proposed sensor

channels were made on the bottom layer in perpendicular direction, along the 3D dome structure for the detection of multidirectional forces (Fig. 1b). The responses to the normal force with respect to the sensor substrate were investigated for the adjustment of sensitivity. As a demonstration, various multidirectional forces were applied with the finger and its corresponding responses were monitored.

Design and working principle

The LM-based multiaxial force sensor is composed of two parts: LM microchannel array with multilayer structure and the dome structure. Multi arrays of liquid metal microchannels are designed for the discrimination of loading location. It is not possible to understand the loaded point or region with only one LM microchannel. Thus, four straight microchannels on the top elastomer layer and another four microchannels on the bottom layer were designed. The number of microchannel in a unit area means the spatial resolution of the sensor. It is possible to measure more accurate signals from various loading angles with more microchannels. In the E-skin application in our research, the area of interest is within 5 mm × 5 mm for the measurement of finger force. Since the minimum feature size of the microchannel using FDM 3D printing process is limited as 500 μm, the maximum number of microchannel was determined as four. Since the top channels and the bottom channels are perpendicular to each other, they comprise four by four matrix for spatial detection of applied forces. Each microchannel has a width of 500 μm and a thickness of 200 μm. Furthermore, the multilayer LM microchannels are shaped into the 3D dome structure. When the morphology of the sensor is a plane or in 2D, it is difficult to detect the tangential loadings and cause a severe shear stress inside. On the other hand, the 3D dome structure can translate the tangential loading to change of cross-sectional area of LM microchannel along the dome. Unlike previous multiaxial force sensors with dome structure [22], the dome structure does not have to be rigid our proposed sensor. Previous multiaxial sensors used a rigid half-spherical structure to deliver external forces to the strain gauges or sensing structures beneath it by torque induced by the tangential force. When LM microchannels are located along the surface of the dome, however, they are directly compressed by the external forces. This enables the sensor to become all-soft structure that can conformally adapted to arbitrary substrates.

All-soft liquid metal-based multiaxial force sensor detects the forces by the change of resistances of multi LM microchannel array. Galinstan, which is an eutectic alloy of gallium, indium, and tin attracts increasing attentions for its excellent mechanical and electrical properties as a component of stretchable electronic applications [23, 24]. Due to its intrinsic properties as a liquid metal, the microchannel filled with Galinstan can easily deformed into 3D dome shape without any mechanical or electrical failure. When there is

an external force applied to the LM microchannel, the cross-sectional area of the microchannel decreases, resulting the increase of the resistance. The responses of each LM microchannel differ with respect to the loading condition.

Liquid metal microchannels of the sensor on the bottom layer were labeled as × 1, x2, x3, and x4 and those on the top layer were as y1, y2, y3, and y4 (Fig. 2a). In cross-sectional view (x–z plane), multidirectional load could be applied to the sensor with the angle θ. When the normal force is loaded (θ = 0°), more force would be delivered to the those LM microchannels at the center: x2, x3, y2, and y3 than those on the side. As θ increases, the response of the sensor would shift from the center to the side, which can be visualized as in Fig. 2b: 1(θ = 0°) → 2(θ = 15°) → 3(θ = 30°). The deformations of the dome structure with respect to the loading angle θ were simulated using finite element method (FEM) (Fig. 2b).

Fabrication process

The LM-based multiaxial force sensor is fabricated by the following procedures (Fig. 3). First, a master mold is designed for the liquid metal microchannel using 3D CAD (Fusion 360, Autodesk). Four microchannels are sharing a single reservoir structure at the end. The reservoir provides a room for the liquid metal injection

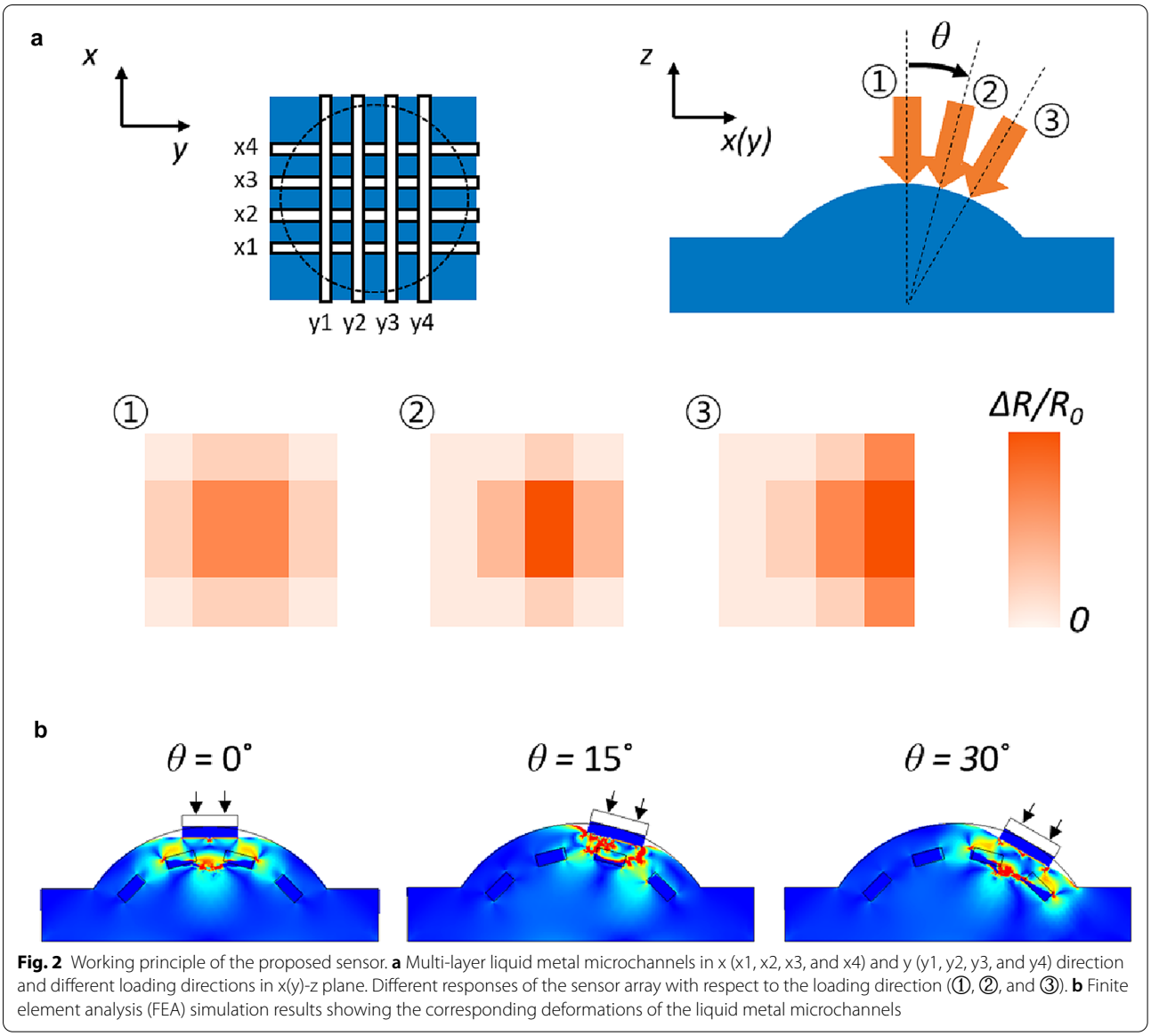

Fig. 2 Working principle of the proposed sensor. **a** Multi-layer liquid metal microchannels in x (x1, x2, x3, and x4) and y (y1, y2, y3, and y4) direction and different loading directions in x(y)-z plane. Different responses of the sensor array with respect to the loading direction (①, ②, and ③). **b** Finite element analysis (FEA) simulation results showing the corresponding deformations of the liquid metal microchannels

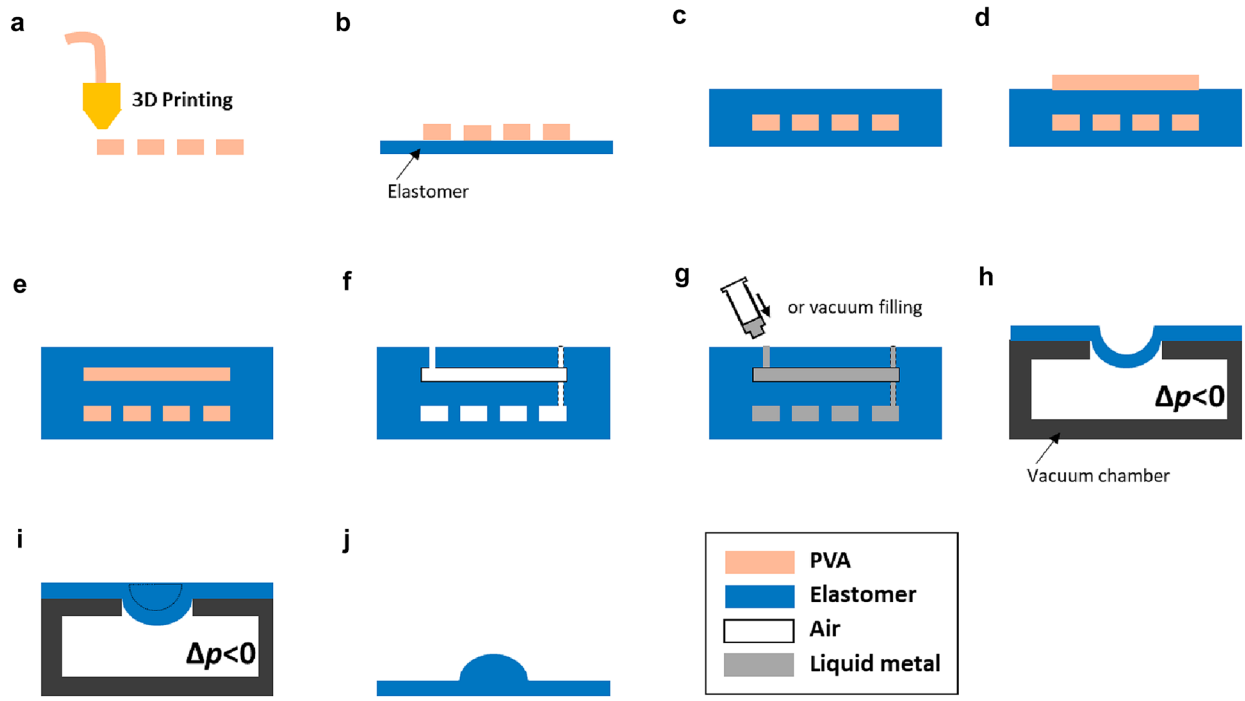

Fig. 3 Fabrication process of the proposed sensor. **a** 3D Printing of microchannel mold. **b** Placement of the 3D-printed PVA mold on the elastomer film. **c** Embedment of the mold by spin coating and curing. **d** Placement of the 2nd mold on the top. **e** Embedment of the mold. **f** Removal of the mold. **g** Filling of liquid metal inside microchannel using syringe injection or vacuum filling. **h** Fabrication of dome structure using the vacuum chamber. **i** Curing of additional elastomer for the fixation of dome structure. **j** Fabrication of the proposed sensor

and stores remaining liquid metals after filling the microchannel. The mold is 3D-printed with poly(vinyl alcohol) (PVA) filament which is a water-soluble material (Fig. 3a). The dimension of the microchannel mold is 500 μm width and 200 μm thickness which is a minimum feature size of fused deposition modeling (FDM) 3D printing. The 3D printed mold is positioned on the elastomer sheet (Fig. 3b). Due to their intrinsic stiction between the mold and the elastomer, the mold is not move during the spin coating process. The mold is then embedded into the elastomer (Dragonskin10, Smooth-on) by spin coating (300 rpm, 60 s), followed by the additional mold embedment (Fig. 3c). The mold on the top layer is aligned perpendicular to that on the bottom so that the microchannels on the top and the bottom can cross each other in a perpendicular direction (Fig. 3d–e). Then, the PVA molds are dissolved by injection of water with at the temperature of 40–50 °C for the fast removal (Fig. 3f) after the PVA removal, the elastomer with empty microchannels is dried at 50 °C for 2 h. Then, Galinstan is injected into the empty microchannels using a syringe injection or vacuum filling method (Fig. 3g). 3D dome structure is fabricated with a vacuum chamber. Vacuum was applied to the crossing area of the liquid metal-filled plane sensor at the hole with a diameter of 5 mm (Fig. 3h). The height of the dome was controlled by the amplitude of applied pressure. When the thickness of the elastomer was 0.8 mm, the height of the dome (H) was 0.9 mm with $\Delta p = -10$ kPa and H = 2.2 mm with $\Delta p = -30$ kPa. To fix the shape of the dome, an additional elastomer was filled and cured on the opposite side of the dome, filling the concave hills (Fig. 3i). After the curing, the pressure is released (Fig. 3j). Electric wires are then directly inserted into each reservoir of the channels for the integration with the circuit system.

Performance characterization

To investigate the response of the multiaxial force sensor, three-axial load cell (SM-50 N, CAS Korea) was implemented for the monitoring of force applied to the sensor in x, y, and z direction and the linear stage with a

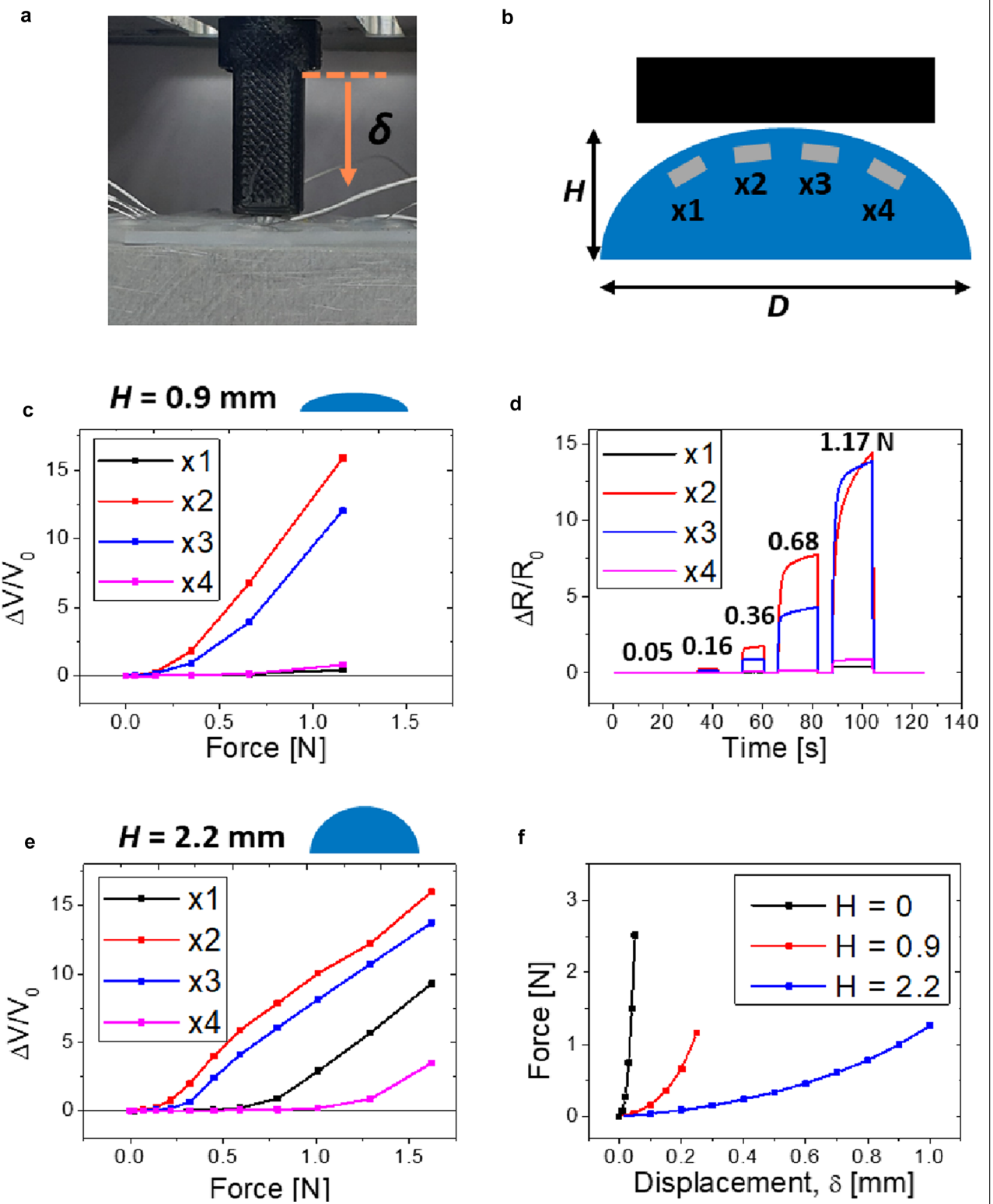

Fig. 4 Performance characterization. **a** Experimental setup. **b** Schematic view of the sensor. (x1–x4: labels for each LM microchannel, *H*: height of the dome, and *D*: diameter of the dome) **c** Response of the sensor with the dome height (*H*) of 0.9 mm to normal directional force. **d** Real-time response to various loadings **e** Response of the sensor when *H* is 2.2 mm. **f** Sensitivity to the displacement according to the height of the dome

loading tip for displacement-controlled loading (Fig. 4a) Each LM microchannel was connected to 8-channel ADC reader (ADS1114, Texas Instruments) installed on Arduino DUE (Arduino). LM microchannels were labeled as x1, x2, x3, and x4 as shown in the Fig. 4b. At the initial state (F = 0), the voltage is approximately 20 mV and its corresponding resistance is about 0.4 Ω owing to the high electrical conductivity of liquid metal. Thanks to the voltage dividing circuit and high resolution ADC reader, the small change in voltage could be monitored.

In the dome sensor, the positions of the inner LM microchannel pair and the outer pair are geometrically symmetric, respectively. (x2 and x3: the inner pair, x1 and x4: the outer pair). Therefore, the sensor responses of each pair under the applied normal force showed a similar tendency. When a normal force of 1.2 N was applied, the relative voltage changes ($\Delta V/V_0$) of the inner pair increased to 12.1 and 15.8, respectively. On the other hand, the responses of x1 and x4 of the outer pair were only 0.4 and 0.8, respectively (Fig. 4c). It means that the developed multiaxial force sensors can distinguish the direction of an applied force by utilizing the difference position of LM microchannel by the change of dome geometry. In addition, the responses of the sensors were recovered to their initial values after various loading cycles owing to the excellent stability of the liquid metal and the structure of the sensor (Fig. 4d). Meanwhile, when the height of the dome (H) increased to 2.2 mm, the outer sensor pair shows slightly different responses: the response of x1 began to increase after 0.5 N, while that of x4 increased after 1 N (Fig. 4e). This is due to the different gap between the LM microchannels along the dome.

Force–displacement curves depending on the various height of the dome were measured to verify the sensitivity of the sensor. When H increases, less force is applied with the same displacement, and the sensitivity of the sensor decreases (Fig. 4f). For example, to apply 1 N of normal force, 200 μm of loading displacement is required for the dome height of $H = 0.9$ mm, while 900 μm of displacement is needed for $H = 2.2$ mm. When the force applied to the sensor without a dome structure ($H = 0$ mm), the response dramatically increases with the loading displacement. As H increases, larger displacement is required for the loading of force. Also, the dome with larger H provides larger radial displacement among the adjacent channels, which leads to different response behavior of the sensor array. These characteristics result in the difference in sensitivity the sensitivity of the multiaxial sensor regarding with respect to the dome height and diameter. In addition, the diameter of the dome would also affect the gap among the liquid metal channels, although not covered in our study.

The characteristics of the developed sensor were investigated on the flat surfaces, where accurate control of the direction and magnitude of the force is possible. On the other hand, when the sensor is located on the curved or wavy surfaces, the trend or behaviour of the sensor would be different because the microchannels are deformed, requiring an additional calibration of the initial state. The characterization of the sensor on different surface geometry is beyond the scope of this study and it is left as the future work for the practical E-skin applications.

Applications: finger loading

To demonstrate the feasibility of the proposed sensor, we applied various directional forces using a finger (Fig. 5a). Various directional forces (F_1–F_4) were consequently applied to the sensor; F_1: (−x, 0, −z), F_2: (+x, 0, −z), F_3: (0, +y, −z), and F_4: (0, −y, −z) (Fig. 5b). To visualize the direction and amplitude of loaded force, we multiplied the relative voltage changes of the top and the bottom array and implemented 4×4 matrix array with 3D colormap (MATLAB, Mathworks). The LM microchannels can be divided into two groups: the top and the bottom layer. There are four LM microchannels on the top layer; x1, x2, x3, and x4, and four on the bottom; y1, y2, y3, and y4. Each component has its own response, or relative voltage change ($X_i = \Delta V_{xi}/V_{xi0}$ and $Y_i = \Delta V_{yi}/V_{yi0}$) and can be summarized as below.

$$X = (X_1, X_2, X_3, X_4)$$

$$Y = (Y_1, Y_2, Y_3, Y_4)$$

$$S = Y^T * X.$$

To detect the direction of loading, the responses of LM microchannels of the top and the bottom are multiplied to build a 4×4 matrix (S). We were able to detect the loading position and their relative magnitude of the force as shown in the Fig. 5c–f.

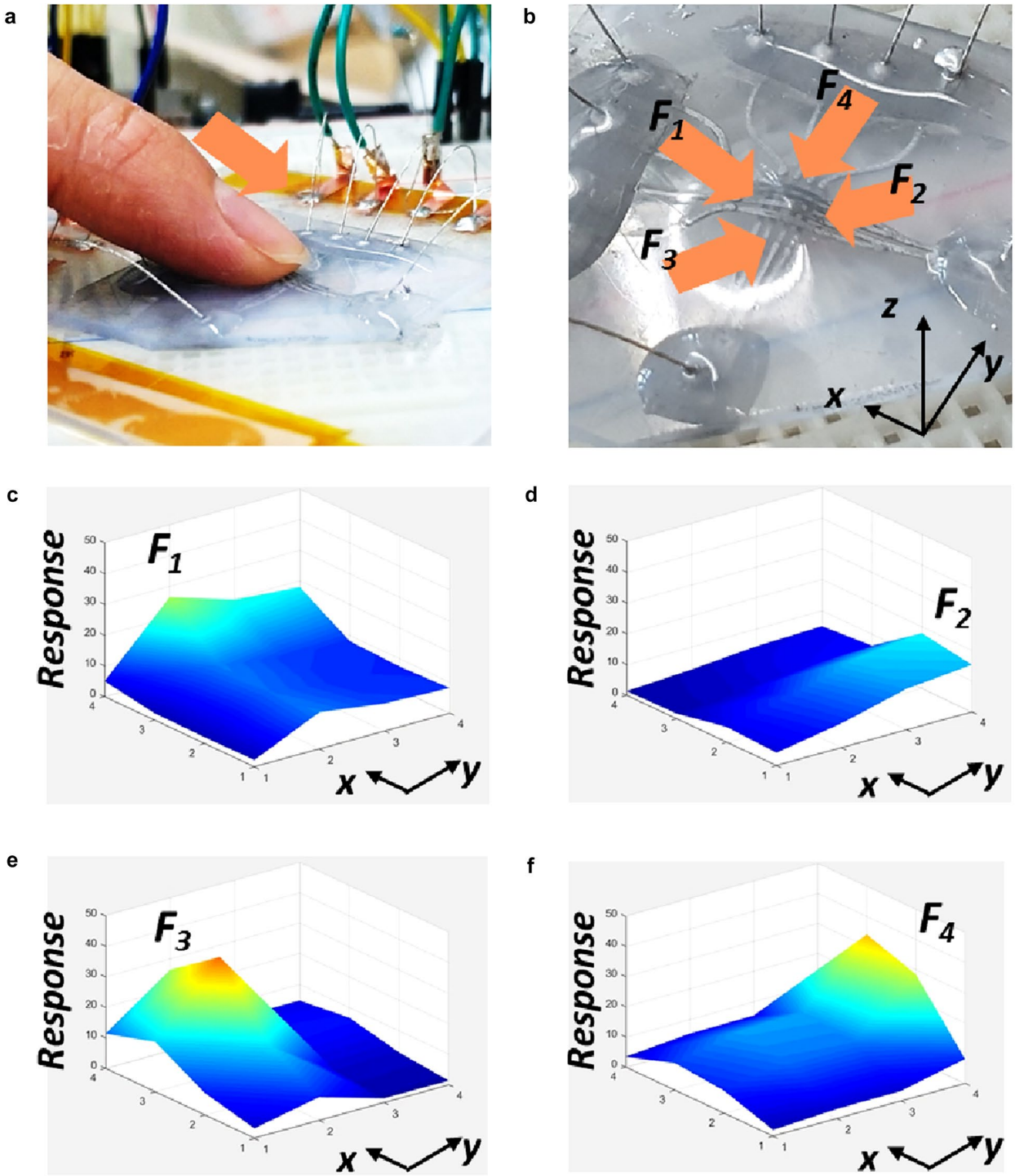

Fig. 5 Application: finger force detection. **a** Image of a finger applying the force. **b** Various loading condition. **c**–**f** Responses to the various loading forces

Conclusion

In this research, we introduce a multidirectional force sensor using liquid metal microchannel array with a dome structure. LM microchannels were fabricated using

3D-printed molding. Since the microchannel arrays were located along the dome structure, which is in three-dimensional shape, various directional forces could be distinguished with high force sensitivity. The sensor showed high signal recovery properties owing to intrinsic electromechanical properties of liquid metal with high flexibility. The various directional forces using force were distinguished by the implication of sensor array and corresponding 3D color map. We expect this technology could be used in various soft material-based applications including electronic skin, soft robotics, and wearable devices.

Acknowledgements
Not applicable.

Authors' contributions
KK designed the principle of the sensor, performed experiments, analyzed the data, and wrote the paper. JA performed the FEA simulation, JC fabricated the dome structure, YJ constructed the experimental system to characterize the multiaxial force sensor, and OG conducted the experiments. IP led the overall direction of the project and wrote the paper. All authors have given their approval to the final version of the manuscript. All authors read and approved the final manuscript.

Funding
This work was supported by a National Research Foundation of Korea (NRF) grant funded by the Korean government (MSIT) (No. 2018R1A2B2004910).

Availability of data and materials
All data generated or analyzed during this study are included in this published.

Competing interests
The authors declare that they have no competing interests.

Author details
[1] Department of Mechanical Engineering, Korea Advanced Institute of Science and Technology (KAIST), 291 Daehak-ro, Yuseong-gu, Daejeon 34141, Republic of Korea. [2] Korea Institute of Machinery and Materials (KIMM), 156 Gajeong-buk-Ro Yuseong, Gu Daejeon, Korea.

Received: 2 August 2020 Accepted: 1 December 2020
Published online: 04 January 2021

References

1. Dargahi J, Najarian S (2004) Human tactile perception as a standard for artificial tactile sensing-a review. Int J Med Robot Comput Assist Surg 01:23. https://doi.org/10.1581/mrcas.2004.010109
2. Hao J, Bonnet C, Amsalem M et al (2014) Transduction and encoding sensory information by skin mechanoreceptors. Pflugers Arch Eur J Physiol 467:109–119. https://doi.org/10.1007/s00424-014-1651-7
3. Kim K, Choi J, Jeong Y et al (2019) Highly sensitive and wearable liquid metal-based pressure sensor for health monitoring applications: integration of a 3d-printed microbump array with the microchannel. Adv Healthc Mater 8:1–10. https://doi.org/10.1002/adhm.201900978
4. Kim S, Amjadi M, Lee TI et al (2019) Wearable, ultrawide-range, and bending-insensitive pressure sensor based on carbon nanotube network-coated porous elastomer sponges for human interface and healthcare devices. ACS Appl Mater Interfaces. https://doi.org/10.1021/acsami.9b07636
5. Choi J, Kwon D, Kim K et al (2020) Synergetic effect of porous elastomer and percolation of carbon nanotube filler toward high performance capacitive pressure sensors. ACS Appl Mater Interfaces 12:1698–1706. https://doi.org/10.1021/acsami.9b20097
6. Choi J, Kwon D, Kim B et al (2020) Wearable self-powered pressure sensor by integration of piezo-transmittance microporous elastomer with organic solar cell. Nano Energy 74:104749. https://doi.org/10.1016/j.nanoen.2020.104749
7. James JW, Pestell N, Lepora NF (2018) Slip detection with a biomimetic tactile sensor. IEEE Robot Autom Lett 3:3340–3346. https://doi.org/10.1109/LRA.2018.2852797
8. Wan Y, Qiu Z, Hong Y et al (2018) A highly sensitive flexible capacitive tactile sensor with sparse and high-aspect-ratio microstructures. Adv Electron Mater 4:1–8. https://doi.org/10.1002/aelm.201700586
9. Yamamoto Y, Yamamoto D, Takada M et al (2017) Efficient skin temperature sensor and stable gel-less sticky ECG sensor for a wearable flexible healthcare patch. Adv Healthc Mater 6:1–7. https://doi.org/10.1002/adhm.201700495
10. Kim K, Park J, Suh J, Hoon SJ et al (2017) 3D printing of multiaxial force sensors using carbon nanotube (CNT)/thermoplastic polyurethane (TPU) filaments. Sensors Actuators A Phys 263:493–500. https://doi.org/10.1016/j.sna.2017.07.020
11. Cho C, Ryuh Y (2016) Fabrication of flexible tactile force sensor using conductive ink and silicon elastomer. Sensors Actuators A Phys 237:72–80. https://doi.org/10.1016/j.sna.2015.10.051
12. Lee YR, Chung J, Oh Y, Cha Y (2019) Flexible shear and normal force sensor using only one layer of polyvinylidene fluoride film. Appl Sci. https://doi.org/10.3390/app9204339
13. Yin J, Santos VJ, Posner JD (2017) Bioinspired flexible microfluidic shear force sensor skin. Sensors Actuators A Phys 264:289–297. https://doi.org/10.1016/j.sna.2017.08.001
14. Matich S, Hessinger M, Kupnik M et al (2017) Miniaturized multiaxial force/torque sensor with a rollable hexapod structure: Miniaturisierter Kraft-Momenten-Sensor auf Basis einer gerollten Hexapod-Struktur. Tech Mess 84:S138–S142. https://doi.org/10.1515/teme-2017-0046
15. Zhao Y, Zhao Y, Ge X (2018) The development of a triaxial cutting force sensor based on a MEMS strain gauge. Micromachines. https://doi.org/10.3390/mi9010030
16. You X, He J, Nan N et al (2018) Stretchable capacitive fabric electronic skin woven by electrospun nanofiber coated yarns for detecting tactile and multimodal mechanical stimuli. J Mater Chem C 6:12981–12991. https://doi.org/10.1039/C8TC03631D
17. Gong S, Wang Y, Yap LW et al (2018) A location- and sharpness-specific tactile electronic skin based on staircase-like nanowire patches. Nanoscale Horizons 3:640–647. https://doi.org/10.1039/c8nh00125a
18. Sun X, Sun J, Li T et al (2019) Flexible tactile electronic skin sensor with 3D force detection based on porous CNTs/PDMS nanocomposites. Nano Micro Lett 11:1–14. https://doi.org/10.1007/s40820-019-0288-7
19. Kwon SN, Kim SW, Kim IG et al (2019) Direct 3D printing of graphene nanoplatelet/silver nanoparticle-based nanocomposites for multiaxial piezoresistive sensor applications. Adv Mater Technol 4:1–9. https://doi.org/10.1002/admt.201800500
20. Wang S, Li Q, Wang B et al (2019) Recognition of different rough surface based highly sensitive silver nanowire-graphene flexible hydrogel skin. Ind Eng Chem Res 58:21553–21561. https://doi.org/10.1021/acs.iecr.9b04947
21. Peng S, Wu S, Yu Y et al (2020) Multimodal capacitive and piezoresistive sensor for simultaneous measurement of multiple forces. ACS Appl Mater Interfaces 12:22179–22190. https://doi.org/10.1021/acsami.0c04448
22. Ji B, Zhou Q, Wu J et al (2020) Synergistic optimization toward the sensitivity and linearity of flexible pressure sensor via double conductive layer and porous microdome array. ACS Appl Mater Interfaces. https://doi.org/10.1021/acsami.0c08910
23. Yang J, Tang D, Ao J et al (2020) Ultrasoft liquid metal elastomer foams with positive and negative piezopermittivity for tactile sensing. Adv Funct Mater 2002611:1–10. https://doi.org/10.1002/adfm.202002611
24. Kim K, Choi J, Jeong Y, et al (2019) Strain-Insensitive Soft Pressure Sensor for Health Monitoring Application Using 3D-Printed Microchannel Mold and Liquid Metal. in 2019 20th International Conference on Solid-State Sensors, Actuators and Microsystems & Eurosensors XXXIII (TRANSDUCERS & EUROSENSORS XXXIII). 2535–2538

Publisher's Note